Synthesis and characterisation of pyrene-labelled polydimethylsiloxane networks: towards the *in situ* detection of strain in silicone elastomers†

Nicholas A. A. Rossi,‡*[a] Elizabeth J. Duplock,[a] Jon Meegan,[b] David R. T. Roberts,[a] Julian J. Murphy,[b] Mogon Patel[b] and Simon J. Holder*[a]

Received 5th May 2009, Accepted 10th July 2009
First published as an Advance Article on the web 2nd September 2009
DOI: 10.1039/b908708g

Pyrene-substituted polyhydromethylsiloxanes (PHMS-Py$_x$) were synthesised by the hydrosilylation reaction of prop-3-enyloxymethylpyrene with polyhydromethylsiloxane ($M_n = 3700$). The ratio of pyrene substituent to Si–H unit was varied to afford a range of pyrene-functionalised polysiloxanes. These copolymers were subsequently incorporated into polydimethylsiloxane (PDMS) elastomers by curing *via* either Pt(0) catalysed hydrosilylation with divinyl-terminated PDMS ($M_n = 186$) and tetrakis(dimethylsiloxy)silane, or Sn(II) catalysed condensation with α,ω-dihydroxyPDMS ($M_n = 26\,000$) and tetraethoxysilane. An alternative method involving the synthesis and integration of [3-(pyren-1-ylmethoxy)propyl]triethoxysilane (Py-TEOS) into PDMS elastomers was also investigated: a mixture of α,ω-dihydroxyPDMS ($M_n = 26\,000$), tetraethoxysilane, and Py-TEOS was cured using an Sn(II) catalyst. Certain of the resulting fluorescent pyrene-labelled elastomers were studied by differential scanning calorimetry and dynamic mechanical analysis. No significant changes were observed in the thermal or mechanical properties of the elastomers containing pyrene when compared to otherwise identical samples not containing pyrene. All of the pyrene-containing elastomers were demonstrated to be fluorescent under suitable excitation in a photoluminescent spectrometer. Two of the elastomers were placed in a photoluminescence spectrometer and subjected to cycles of extension and relaxation (strain = 0–16.7%) while changes in the emission spectra were monitored. The resulting spectra of the elastomer containing the PHMS-Py$_{50}$ copolymers were variable and inconsistent. However, the emission peaks of elastomers containing Py-TEOS displayed clear and reproducible changes in fluorescence intensity upon stretching and relaxation. The intensity of the monomer and excimer emission peaks was observed to increase with elongation of the sample and decrease upon relaxation. Furthermore, the ratio of the intensities of the excimer : monomer peak decreased with elongation and increased with relaxation. In neither case was there appreciable hysteresis, suggesting that fluorescent labelling of elastomers is a valid approach for the non-invasive *in situ* monitoring of stress and strain in such materials.

1. Introduction

The incorporation of fluorophores into polymeric materials has led to a number of end-user applications including light emitting diodes,[1,2] pressure-sensitive paints,[3,4] and thin film chemosensors.[5] Furthermore, investigations into methods whereby strain and deformation can be quantifiably measured using optical properties have led to interest in the development of fluorescent stress–strain sensors.[6–8] The concept of correlating optical properties with deformation is based on the following rationale: as an elastomer doped with a fluorophore undergoes deformation, changes in the polymer tensile state alter the local environment of the fluorophore. The change in environment and extent of deformation can then be measured spectroscopically. Fluorophores, such as pyrenes or carbazoles,[9,10] form excimers and can be used to follow changes in properties such as the architecture, film thickness, concentration, and morphology of a polymeric system. By correlating these properties with the intensity and wavelength of fluorescence, it is possible in principle to measure and predict certain physical changes and events such as mechanical failure. Fluorescent materials have a distinct advantage over other optically active materials and optical techniques since emission can be measured at the surface of polymer-coated objects. The non-destructive and non-invasive nature of fluorescence spectroscopy means deformation can be

[a]*Functional Materials Group, School of Physical Sciences, University of Kent, Canterbury, Kent, UK CT2 7NH. E-mail: S.J.Holder@kent.ac.uk; nick@rossi.net*
[b]*AWE, Reading, Berkshire, UK RG7 4PR*

† Electronic supplementary information (ESI) available: Fig. S1: (a) ^{1}H NMR and (b) ^{13}C NMR spectra of prop-3-enyloxymethylene in $CDCl_3$. Fig. S2: FT-IR spectra of PHMS-Py$_{50}$ and PHMS-Py$_{100}$. Fig. S3: (a) ^{1}H and (b) ^{13}C NMR spectra of [3-(pyren-1-ylmethoxy)propyl]triethoxysilane (Py-TEOS) in $CDCl_3$. Fig. S4: stress–strain plots from DMA of PHMS-Py$_x$ and Py-TEOS containing elastomers measured at 40 °C. Table S1: thermal transitions for elastomer samples recorded on first heating run at 10 °C min^{-1}. Fig. S5: UV-vis spectra of PHMS-Py$_{50}$ and 1-pyrenemethanol in THF. Procedure for Soxhlet extraction. Fig. S6: comparison of photoluminescent spectra of Sn7 (Py-TEOS), Pt13 (PHMS-Py$_{50}$) and Pt16 (PHMS-Py$_{100}$) before and after Soxhlet extraction with THF. See DOI: 10.1039/b908708g

‡ *Current address*: University of British Columbia, Center for Blood Research, Department of Pathology & Laboratory Medicine, Vancouver, BC, Canada V6T 1Z3.

measured *in situ*. For example, mechanical strain sensing on polystyrene/polyisoprene networks has been observed using strain probes based on carbazole compounds.[7] To our knowledge, an accurate system has yet to be developed since data are difficult to reproduce without a relatively large degree of error.

Although polysiloxane-based elastomers are found in numerous applications ranging from elastomeric sealants to contact lenses,[11] examples of fluorescent polysiloxanes are relatively rare.[12] A non-destructive means of analysing the mechanical response of such materials to stress *in situ* is highly desirable and could be expected to find widespread use. The combination of pyrene with polysiloxane *via* the hydrosilylation of poly(methylhydrosiloxane) (PHMS) with vinyl-functionalised 1-ethylpyrene was reported in 1995 by Bisberg *et al.*[2] The 1-ethylpyrene precursor had a fluorescence emission centred around 400 nm and upon attachment to the polysiloxane backbone, a bathochromically shifted emission peak around 490 nm was observed indicative of excimer formation. Other examples of the incorporation of pyrene and also vinyl-functionalised carbazoles onto polysiloxanes have also been demonstrated.[13] The fluorescence properties of telechelic, pyrene-labelled PDMS films were measured as a function of film thickness and temperature,[14] achieved by measuring the ratio of excimer to monomer intensities (I_E/I_M) which decreased as film thickness decreased. Other reports describe pyrene-doped epoxy resins which were used to measure the change in fluorescence as a function of deformation,[8] while pyrene fluorescence has routinely been used to detect the extent of micelle formation.[15,16] Polymers such as polyethylene,[17,18] poly(methyl methacrylate),[19] polystyrene,[20] and polysiloxanes[2] have incorporated pyrene as either a marker or a probe.

In this paper, the synthesis of a simple fluorescent elastomer system based on pyrene labels suitable for the non-invasive, *in situ* monitoring of strain in an elastomer is presented. The relatively long singlet excited state fluorescence lifetime and high fluorescence quantum yield of pyrene make it an ideal choice of fluorophore.[21] One disadvantage of simply incorporating pyrene into a polymeric matrix is that the limited solubility/miscibility of pyrene can lead to phase separation in the matrix and furthermore pyrene has been shown to leach from polymeric matrices severely hampering the lifetime and reproducibility of such systems.[22] Consequently the covalent attachment of pyrene to an elastomer matrix was necessary. A further requirement for a non-invasive fluorescent probe in real-world applications is that the inclusion of the probe does not significantly alter the physical properties of the elastomer and must therefore be included at very low concentrations in a non-intrusive manner. Two approaches for synthesising functionalised pyrene molecules and macromolecules suitable for incorporation into polydimethysiloxane-based elastomers are described. Firstly, allyl functionalised pyrene was conjugated onto short PDMS chains *via* hydrosilylation and subsequently incorporated into elastomeric networks *via* cross-linking through further hydrosilylation. Secondly, a triethoxysilane functionalised pyrene cross-linker molecule was synthesised and incorporated into elastomeric networks formed using Sn(II) catalysts. The structures of the precursor molecules and polymers were confirmed using NMR spectroscopy and gel permeation chromatography (GPC), while a comparison of the physical and thermal properties of the resulting networks was carried out using differential scanning calorimetry (DSC) and dynamic mechanical analysis (DMA). The fluorescent response of these materials under applied stress suggests this simple fluorescent elastomer system could potentially be suitable for the non-invasive, *in situ* monitoring of strain in an elastomer.

2. Experimental

2.1 Materials

1-Pyrenemethanol (98%), acryloyl chloride (98%), allyl bromide (99%), Karstedt's catalyst (platinum(0)-1,3-divinyl-1,1,3,3-tetramethyldisiloxane complex, 3 wt% solution in xylenes), triethoxysilane (95%), triethylamine (99%), sodium hydride (60% dispersion in mineral oil), and poly(hydromethylsiloxane) (M_n = 1700–3200 in product literature, M_n = 3700 by end-group analysis *via* ^{1}H NMR) were purchased from Aldrich and used as received. Hydroquinone (99% (HPLC), Fluka), silica gel 60 (0.040–0.063 mm, 230–400 mesh, Lancaster), polydimethylsiloxane silanol-terminated (DMS-S31) (M_w 26 000, ABCR), tetrakis(dimethylsiloxy)silane (TDSS) (97%, ABCR), tin(II) 2-ethylhexanoate (95%, Sigma), and vinyldimethylsiloxy terminated polydimethylsiloxane (DMS-V00) (M_w 186, ABCR) were used as received.

Dichloromethane (AR grade), acetonitrile (AR, anhydrous), ethyl acetate (AR grade), hexane fraction from petroleum (LR grade), and methanol (AR grade) were used as received from Fischer. Tetrahydrofuran was pre-dried over magnesium sulfate and sodium wire, then distilled over benzophenone immediately prior to use. Toluene was pre-dried over magnesium sulfate and sodium wire, then distilled over sodium wire immediately prior to use.

2.2 Apparatus

^{1}H, ^{13}C and ^{29}Si nuclear magnetic resonance (NMR) spectra were recorded at 30 °C using a JEOL GX-270 spectrometer from solutions in $CDCl_3$. Infra-red spectra were collected using a Thermo Nicolet Avatar 360 FT-IR spectrometer. UV-vis spectroscopic analysis was performed on a UNICAM UV-500 UV-visible spectrometer. Excitation and emission spectra were collected using a Varian CARY Eclipse fluorescence spectrophotometer and a Perkin Elmer LS 50 B luminescence spectrometer. Mixing of the elastomer mixtures was achieved using a NuSil corporation DAC 150FV2-K Speedmixer. Freeze drying was carried out using a Heo Drywinner. Thermal analysis was carried out on a TA Instruments DSC2910 calibrated with indium. Dynamic mechanical analysis (DMA) was performed on *ca.* 10 mm diameter and 2 mm deep spherical pad of PDMS material using a TA instruments DMA Q800 instrument fitted with a compression head. All reactions were carried out under dry, inert conditions using Schlenk-line techniques. Elastomers were formed in PTFE circular moulds (mould diameter = 6.0 cm, height = 0.2 cm).

2.3 Syntheses

2.3.1 Prop-3-enyloxymethylpyrene. 1-Pyrenemethanol (4.00 g, 0.0172 mol) and sodium hydride in mineral oil (NaH, 1.03 g,

0.0258 mol) were added to a 100 ml dry 50 : 50 toluene–tetrahydrofuran mixture in a 250 ml round-bottomed flask fitted with a condenser. The mixture was heated to 70 °C. After 2 h, the solution was cooled and allyl bromide (3.12 g, 0.0258 mol) was added dropwise *via* a syringe. The mixture was then heated to 70 °C and heated for 24 h. After cooling, excess sodium hydride was removed by the addition of methanol. The solution was filtered and toluene evaporated off. Excess starting material was removed *via* a silica gel column using a 50 : 50 mixture of ethyl acetate and hexane. In these solvents the product had an R_f value of 0.64. Mineral oil was removed by dissolving the product in acetonitrile (20 ml) and washing with hexane (4 × 15 ml). The product was obtained as a yellow oil in 49% yield.

δ_H (270 MHz; $CDCl_3$): 4.19 (dt, 2H, OCH_2, $J = 5.68$, 1.48 Hz); 5.25 (s, 2H, CH_2O); 5.30 ppm (ddt, 1H, CHCH^{cis}H^{trans}, $J = 9.76$, 1.73, 1.24 Hz); 5.41 ppm (qd, 1H, CHCH^{cis}H^{trans}, $J = 17.23$, 1.61 Hz); 6.08 ppm (ddt, 1H, CHCHH, $J = 16.06$, 10.37, 5.68 Hz); 8.01 ppm (m, 4H, *ArH*); 8.16 ppm (m, 4H, *ArH*); 8.37 ppm (d, 1H, *ArH*, $J = 9.26$ Hz). δ_C (68 MHz; $CDCl_3$): 70.61 ppm (OCH_2); 71.27 ppm (CH_2O); 117.41 ppm ($CHCH_2$); 123.43–131.42 ppm (15 Ar*C*); 131.42 ppm (Ar*C*CH_2); 134.81 ppm (CH_2CH).

In a modified method a procedure identical to that outlined above was followed but using NaH powder in place of the NaH in mineral oil suspension. The product was obtained as a yellow oil in 71% yield (4.18 g).

2.3.2 Poly(hydromethylsiloxane-*co*-methyl(propoxymethylpyrenyl)siloxane) (PHMS-Py$_x$). Prop-3-enyloxymethylpyrene (0.30 g, 0.0011 mol) was added to a solution of PHMS (M_n 1700–3200; 0.0883 g, 2.39×10^{-5} mol) in toluene (10 ml). Karstedt's catalyst solution (10 μl, 6.7×10^{-7} mol) was added and the solution was then heated to 75 °C. After 4 h, the toluene was removed under reduced pressure. The product was purified by dissolving in a minimum amount of acetonitrile and precipitating in hexane. A centrifuge was used to separate the product (which formed a suspension in hexane). The procedure was repeated to synthesise a range of PHMS-*co*-Py$_x$ copolymers containing various Si–H to pyrene molar ratios (Table 1).

δ_H (270 MHz; $CDCl_3$): 0.0 (s, 3H, SiCH_3); 0.5 (t, 2H, SiCH_2); 3.3 (m, 2H, $CH_2CH_2CH_2$); 3.3 (t, 2H, CH_2CH_2O); 4.7 (s, 2H, OCH_2); 4.7 (s, 1H, Si*H*); 7.4–8.3 (m, 9H, Ar*H*). δ_C (67.8 MHz; $CDCl_3$): 0 (SiCH_3); 13 (SiCH_2); 24 ($CH_2CH_2CH_2$); 72 (CH_2CH_2O); 74 (OCH_2C); 122–134 (Ar*C*).

2.3.3 [3-(Pyren-1-ylmethoxy)propyl]triethoxysilane. Triethoxysilane (0.43 g, 0.48 ml, 0.0026 mol) and prop-3-enyloxymethylpyrene (1.05 g, 0.0039 mol) were added to dry toluene (20 ml) in a 100 ml round-bottomed flask fitted with a condenser. Karstedt's catalyst solution (10 μl, 6.7×10^{-7} mol) was added to the solution which was heated to 70 °C overnight. Toluene was removed under reduced pressure and the mixture was flushed through a small silica column to remove starting material and catalyst. Analysis by TLC showed the presence of isomeric material, which was removed *via* a silica gel column using dichloromethane as the eluent.

δ_H (270 MHz; $CDCl_3$): 0.96 ppm (t, 2H, SiCH_2, $J = 8.28$ Hz); 1.19 ppm (t, 9H, OCH_2CH_3, $J = 7.04$ Hz); 1.79 ppm (q, 2H, $SiCH_2CH_2$, $J = 6.67$–6.79 Hz); 3.60 ppm (t, 2H, $SiCH_2CH_2CH_2$, $J = 6.67$ Hz); 3.78 ppm (q, 6H, OCH_2CH_3, $J = 6.92$ Hz); 5.21 ppm (s, 2H, ArCH_2O); 8.01 ppm (m, 4H, *ArH*); 8.16 ppm (m, 4H, *ArH*); 8.37 ppm (d, 1H, *ArH*, $J = 9.26$ Hz). δ_C (67.8 MHz; $CDCl_3$): 6.99 ppm (SiCH_2); 18.63 ppm (OCH_2CH_3); 23.54 ppm ($SiCH_2CH_2$); 58.69 ppm ($SiCH_2CH_2CH_2$); 71.75 ppm (OCH_2CH_3); 73.14 ppm (ArCH_2O); 123.67–132.21 ppm (15Ar*C*); 132.21 ppm (Ar*C*CH_2).

2.3.4 PDMS elastomers. The appropriate PDMS (silanol or vinyl-terminated) (9.00 g, 3.46×10^{-4} mol), pyrene-labelled compound (Py-TEOS or PHMS$_x$Py$_y$), cross-linking agent (TEOS or TDSS) and catalyst (tin(II) 2-ethylhexanoate or Karstedt's catalyst) were added to a plastic beaker and speed-mixed (3600 rpm) for 10–20 s before being poured into a circular Perspex mould. The material was isostatically pressed under 5 tonnes of applied pressure for 10 min before the clear, homogeneous elastomer was removed. The elastomers were stored in zip-lock plastic bags filled with argon. The exact quantities of material used in each preparation are given in Table 2.

Table 1 Pyrene functionalised polyhydromethylsiloxanes

Copolymer	SiH[a] (%)	Pyrene[a] (%)	Solubility[b]
PHMS-Py$_{10}$	90	10	Insoluble
PHMS-Py$_{50}$	50	50	Soluble
PHMS-Py$_{80}$	20	80	Soluble
PHMS-Py$_{90}$	10	90	Soluble
PHMS-Py$_{100}$	0	100	Soluble

[a] Molar unit percentage. [b] In THF and $CDCl_3$.

2.4 Fluorescence spectroscopy of elastomers

The elastomers were cut into rectangles of approximately 10 mm by 22 mm, and clamped to an apparatus which enabled the elastomer strips to be held in place within the fluorimeter at an angle 45° to the incident beam. The apparatus, which consisted of a clamp stand and a Micro Vice Holder (S. T. Japan-EuropeGmBH) was used to stretch (15 mm between clamps) the elastomer films by measurable 0.5 mm increments from 0–2.5 mm (0–16.7% strain).

2.5 Mechanical analysis (DMA)

Materials were analysed for stress–strain behaviour at 25 °C and 40 °C using DMA based, controlled compression release cycling. The test was conducted using a 1 cm diameter disk of material at room temperature (25 °C). A low preload strength (0.05 N) was applied to the sample prior to ramping the force to 18 N at a rate of 3 N min^{-1}, followed by allowing the applied force to return to 0.05 N at a rate of 3 N min^{-1}.

2.6 Thermal analysis (DSC)

DSC traces were collected on as-prepared samples (*ca.* 10 mg) of material hermetically sealed in Al DSC pans. Samples were referenced to an empty pan and the temperature scale was calibrated to an indium standard between −150 and 300 °C. The sample cell was cooled to *ca.* −170 °C using liquid nitrogen at 10 °C min^{-1} and the instrument was set to collect data from −150 to 50 °C on the first heating scan, ramping T at 10 °C min^{-1}.

Table 2 Compositions and appearance of PDMS elastomers

Elastomer[a]	Pyrene component	Weight percent[b]	Initial Appearance	PDMS	TEOS	TDSS	Catalyst
Sn1	PHMS-Py_{50}	0.01	Clear	α,ω-HO, 9.00 g, 3.46×10^{-4} mol	0.14 g, 6.72×10^{-4} mol	—	Tin(II) 2-ethylhexanoate, 0.347 g, 8.57×10^{-4} mol
Sn2	PHMS-Py_{50}	0.05	Clear				
Sn3	PHMS-Py_{50}	0.1	Clear				
Sn4	PHMS-Py_{50}	0.5	Clear, yellow				
Sn6	Py-TEOS	0.01	Clear	α,ω-HO, 9.00 g, 3.46×10^{-4} mol	0.14 g, 6.72×10^{-4} mol	—	Tin(II) 2-ethylhexanoate, 0.347 g, 8.57×10^{-4} mol
Sn7	Py-TEOS	0.05	Clear				
Sn8	Py-TEOS	0.1	Clear				
Sn9	Py-TEOS	0.5	Clear				
Sn10	None	0—Blank	Clear				
Pt12	PHMS-Py_{50}	0.02	Clear, brown	α,ω-Vinyl, 2.00 g, 0.0107 mol	—	7.05 g, 0.022 mol	Karstedts catalyst (20 μl, 1.3×10^{-8} mol)
Pt13	PHMS-Py_{50}	0.2	Bubbles, brown				
Pt14	PHMS-Py_{50}	1.0	Opaque, yellow				
Pt15	None	0—Blank	Clear				
Sn16	PHMS-Py_{100}	2.0	Clear, yellow	α,ω-HO, 9.00 g, 3.46×10^{-4} mol	0.14 g, 6.72×10^{-4} mol	—	Tin(II) 2-ethylhexanoate, 0.347 g, 8.57×10^{-4} mol
Sn17	PHMS-Py_{80}	0.01	Clear				
Sn18	PHMS-Py_{80}	0.1	Clear, yellow				

[a] Sn(II) cured elastomers Sn1–Sn10, Sn16–Sn19; $PDMS(OH)_2$ (9.0 g), TEOS (0.14 g), Sn catalyst (0.347 g) and pyrene-containing compound (PHMS-Py_x or Py–TEOS). Pt(0) cured elastomers Pt11–Pt15; $PDMS(vinyl)_2$ (4.5 g), TDSS (0.2 g), Karstedt's catalyst (20 μl) and percentage of PHMS-Py_{50}. [b] Weight percentage of pyrene based on total weight percentage of PDMS present.

3. Results and discussion

3.1 Synthesis and characterisation of prop-3-enyloxymethylpyrene

The chemical bonding of the pyrene moiety to the siloxane elastomer network is especially important for *in situ* measurements since non-covalently bonded pyrene molecules are known to migrate through and leach from polymeric materials,[22] and therefore the content and homogeneity of the material would not remain constant over a period of time. With the expressed aim of chemically attaching fluorophores into a cross-linked network, polysiloxane copolymers containing both reactive Si–H sites and pyrene moieties were synthesised. There are several methods whereby functional groups can be attached to polysiloxane backbones, including dehydrocoupling, hydrosilylation, and solvolysis reactions. For dehydrocoupling reactions, an Si–H containing polymer such as poly(hydromethylsiloxane), PHMS, is reacted with 1-pyrenemethanol in the presence of platinum, boron, or rhodium catalyst.[23] This methodology was not followed here since the Si–O–C linkages connecting the siloxane backbone with the pyrene moieties can undergo hydrolytic cleavage over time. For most medium to long-term monitoring of strain in elastomers, such potential sites of instability need to be avoided. Hence, the

Scheme 1 Synthesis of prop-3-enyloxymethylene, pyrene-polyhydromethylsiloxane (PHMS-Py_x) copolymers and [3-(pyren-1-ylmethoxy)propyl]triethoxysilane (Py-TEOS).

main focus of the synthetic work presented here involves hydrosilylation reactions, whereby pyrene is attached *via* a substantially more stable Si–C bond. To this end an allyl-functionalised pyrene, prop-3-enyloxymethylpyrene, was synthesised by the addition of allyl bromide to deprotonated 1-pyrenemethanol (Scheme 1). Purification was achieved using flash chromatography and the structure was confirmed using ^{1}H and ^{13}C NMR spectroscopy (ESI†, Fig. S1).

3.2 Synthesis of poly(hydromethylsiloxane-*co*-methyl(propoxymethylpyrenyl)siloxane)s (PHMS-Py$_x$)

A range of copolymers (PHMS-Py$_{10}$ to PHMS-Py$_{90}$) were synthesised by reacting prop-3-enyloxymethylpyrene with PHMS (M_n = 3700) in the presence of a Pt catalyst (Scheme 1). By varying the molar ratio of prop-3-enyloxymethylpyrene to Si–H groups in the PHMS from 0.1 : 1 to 1 : 1, the percentage of Si–H sites in the final copolymers could be varied from 0–90% (Table 1). The resulting crude polymers were purified by passing the reaction mixture through a short silica column to remove the platinum catalyst. Toluene was removed before dissolving the polymer in acetonitrile and precipitating into hexane. In all cases gel-like solids were formed, and often had to be centrifuged in order to separate them from the solvent mixture. By reprecipitating the copolymer three or four times, products (PHMS-Py$_x$) containing no unattached pyrene (as determined by ^{1}H and ^{13}C NMR) were recovered. Impurities removed from the final product included unreacted pyrene and an isomer, prop-2-enyloxymethylpyrene, which is known to form during Pt-catalysed hydrosilylation reactions.[24] Unfortunately, the synthesis of 10% pyrene-substituted PHMS (PHMS-Py$_{10}$) gave a predominantly insoluble material during the purification process. The relatively high abundance of Si–H groups and the presence of platinum catalyst promote cross-linking especially when exposed to air.

PHMS-Py$_{50}$, PHMS-Py$_{80}$, PHMS-Py$_{90}$ and PHMS-Py$_{100}$ did not fully precipitate from hexane and did not separate easily from the solvent mixture; consequently some product was lost during purification resulting in relatively low yields (~50%) of the products. ^{1}H and ^{13}C NMR spectroscopy confirmed the structure and purity (typical NMR spectra are shown in Fig. 1). Since the Si–H groups have a ^{1}H NMR shift around 4.7 ppm, they are obscured by overlapping OCH_2–Py peaks from the substituted pyrene compounds. Therefore it was difficult to determine the exact percentage of Si–H groups remaining along the backbone without a certain degree of error. Comparison of the integrals from the pyrene aromatic peaks to the methyl polysiloxane peaks gave an indirect determination of the presence of Si–H but it must be emphasised that this is only an estimate. Potential side reactions such as hydrolysis or condensation catalysed by Pt occurring at Si–H groups can lead to an incorrect calculation of Si–H. Furthermore the crude materials were passed through a short silica column in order to remove Pt which could also lead to SiH groups being hydrolysed since silica is hydrophilic.

FT-IR spectroscopy displayed distinctive peaks at 2153 cm^{-1} (Si–H stretch) for all polymers where an excess of PHMS was reacted with the allyl-functionalised pyrene PHMS-Py$_{50}$, PHMS-Py$_{80}$, PHMS-Py$_{90}$ (typical spectrum is given in ESI†, Fig. S2). Where substitution of PHMS approached 100% (PHMS-Py$_{100}$) only a minimal Si–H signal was observed. However, the FT-IR spectrum of PHMS-Py$_{50}$ (Fig. S2†) shows that this polymer contains a lot of SiOH groups (the broad band at about 3300 cm^{-1}) and the SiOSi band is much broader than the one found in PHMS-Py$_{100}$ which can be indicative of some degree of polymer cross-linking. A full understanding of the degree of substitution and the final nature of the polymeric materials could be obtained through ^{29}Si NMR analysis which was unfortunately not conducted. Future syntheses of these materials will be subject to more rigorous analysis.

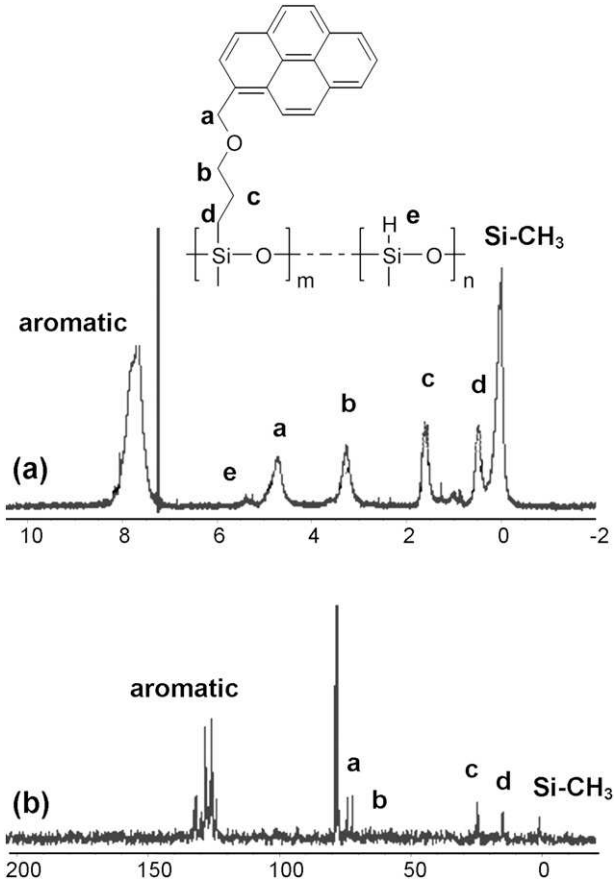

Fig. 1 (a) ^{1}H and (b) ^{13}C NMR spectra of pyrene-polyhydromethylsiloxane (PHMS-Py$_{80}$).

3.3 Synthesis of triethoxy functionalised pyrene, [3-(pyren-1-ylmethoxy)propyl]triethoxysilane (Py-TEOS)

To investigate the fluorescent properties of elastomers containing fluorophores at the cross-linking sites (as opposed to those existing as side groups along the polymer backbone), a pyrene molecule functionalised with TEOS was synthesised. Following a previously published method,[25] pyrene was functionalised with a suitable alkoxysilane group. In order for pyrene to be incorporated into the Sn(II) catalysed condensation reaction, hydrosilylation of prop-3-enyloxymethylpyrene with triethoxysilane (Scheme 1) to give [3-(pyren-1-ylmethoxy)propyl]triethoxysilane (Py-TEOS) was carried out. The compound was purified by flash chromatography using dichloromethane as the eluent and obtained in 49% yield. By varying the method slightly and

employing solid NaH the yields were increased to 71% by removing the need to remove the mineral oil from the crude product. Characterisation was carried out *via* ^{1}H and ^{13}C NMR spectroscopy (ESI†, Fig. S3).

3.4 PDMS elastomer synthesis—Sn catalysed condensation method

Elastomers were synthesised following two methodologies, *via* Sn(II)-catalysed condensation of hydroxyl-terminated polydimethylsiloxane ($PDMS(OH)_2$) or *via* Pt(0)-catalysed hydrosilylation of vinyl-terminated polydimethylsiloxane ($PDMS(vinyl)_2$).[26] In the first instance, Sn(II)-cured elastomers were synthesised by reacting $PDMS(OH)_2$ with a tetraethoxysilane (TEOS) cross-linker (Scheme 2) and an appropriate amount of pyrene-containing polymer, PHMS-Py_x. Addition of THF was necessary to ensure that the copolymer fully dissolved in the mixture. The second method involved Sn(II) catalysed cross-linking of $PDMS(OH)_2$ with Py-TEOS (Scheme 3). In both cases, careful and thorough mixing of the precursor components was required to form homogeneous, clear elastomers since gelation occurred fairly rapidly (~30 s). All components were therefore thoroughly mixed immediately after catalyst addition using a speed-mixer. Perspex moulds were used to form circular elastomers of uniform thickness (~0.2 cm). During gelation, 5 tonnes of pressure were applied in order to remove air bubbles and imperfections. Initially, it was observed that the elastomers would become opaque after exposure to air for several days. Elastomer opacity can be caused by the presence of evolved organics such as ethanol which remain trapped in the material and give localised differences in the refractive index of the material. Continued evolution of ethanol from the ongoing reaction

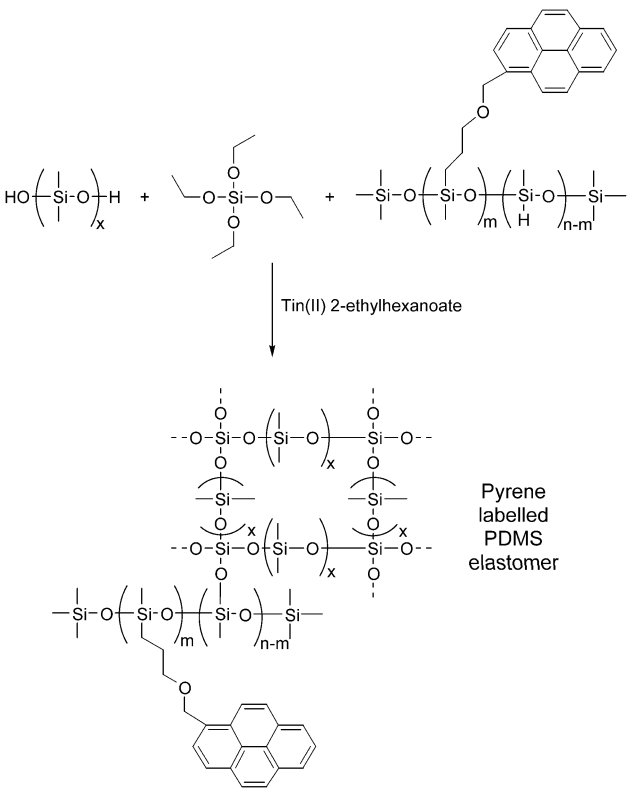

Scheme 2 Synthesis of Sn(II) cured PHMS-Py_x containing elastomers.

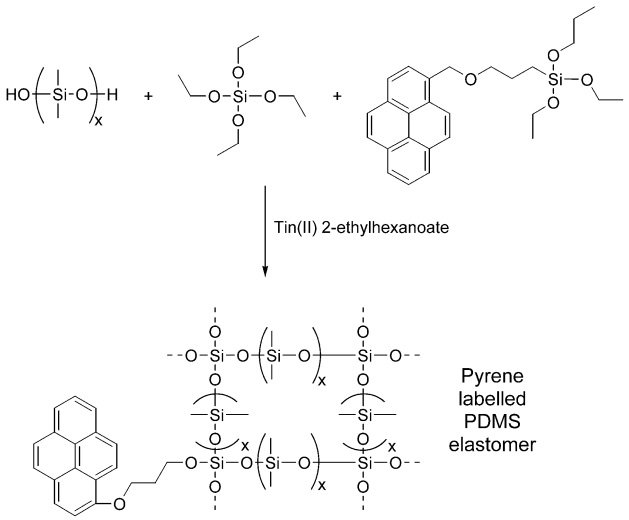

Scheme 3 Synthesis of Sn(II) cured Py-TEOS containing elastomers.

of TEOS can also occur, forming areas of denser silica gel within the elastomer. Attempts to eradicate this effect were made by reducing the concentrations of cross-linker (TEOS) and catalyst. However, this resulted in elastomers which had not been fully cross-linked and instead yielded very viscous liquids. After these initial observations, it was possible to obtain clear elastomers by storing them under inert atmospheres immediately after setting by placing the elastomers in zip-lock bags flushed with argon. Although some opacity developed, the elastomer remained much clearer than the analogous elastomers which had been left out in the atmosphere and remained so after prolonged periods of time (>12 months).

The pyrene-substituted polysiloxane copolymers PHMS-Py_{50}, PHMS-Py_{80}, and PHMS-Py_{100} were incorporated at varying weight percentages (0.01–2.0 wt%, Sn1–Sn4 and Sn16–Sn19, Table 2) into the cross-linking process to form a number of homogeneous polysiloxane elastomers. The pyrene cross-linker, Py-TEOS, was incorporated at similar weight contents to the PHMS-Py_x copolymers to a further series of homogeneous polysiloxane elastomers (Sn6–Sn10).

3.5 PDMS elastomer synthesis—Pt-catalysed hydrosilylation method

Siloxane-based elastomers were also formed *via* Pt(0) catalysed hydrosilylation reactions by mixing vinyl-terminated polydimethylsiloxane ($PDMS(vinyl)_2$) with an excess of tetrakis(dimethylsiloxy)silane (TDSS) cross-linker (Scheme 4). Pyrene-containing polysiloxane chains were incorporated into the elastomer formation process by adding THF solutions of PHMS-Py_{50} to the precursor mix of $PDMS(vinyl)_2$ at three concentrations (Pt12–Pt14, Table 2). The components were mixed using a speed-mixer to form a homogeneous viscous liquid which was poured into a Teflon mould (Perspex moulds could lead to reactions with the mould substrate in this case). The mould was left to set for 10 min while isostatically pressed under 5 tonnes of applied pressure. The resulting elastomers were stored in zip-lock plastic bags filled with argon to prevent any reaction with moisture in the air. Unlike the Sn catalysed TEOS cross-linked elastomers, the vinyl-cured elastomers did not

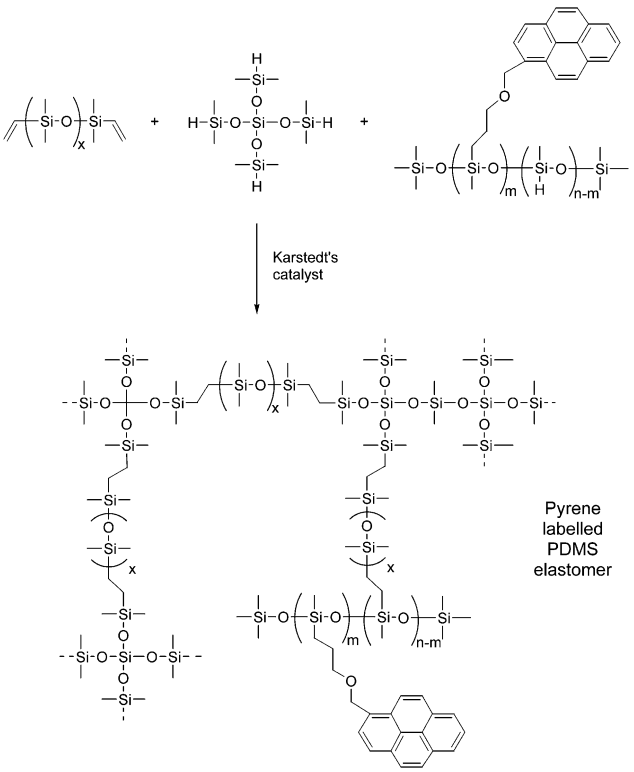

Scheme 4 Synthesis of Pt(0) cured PHMS-Py$_x$ containing elastomers.

become opaque over time. However, as increasing concentrations of copolymer were introduced into the elastomers they became less clear and displayed imperfections caused by effervescence. Thus, while Pt12 (0.02 wt% PHMS-Py$_{50}$) was clear, Pt13 (0.2 wt% PHMS-Py$_{50}$) had clear bubbles in the elastomer and Pt14 was entirely opaque. This is most likely a result of hydrogen evolution or rapid curing leading to trapped air. The elastomers were also light brown or dark yellow in colour due to the presence of residual platinum complexes.

3.6 Mechanical analysis

Thermal and mechanical analysis was performed on several samples in order to obtain preliminary data regarding the nature of the elastomers formed using either Pt(0) or Sn(II) cross-linking systems. DMA was used to measure the stiffness, hysteresis and recovery properties of the elastomers containing pyrene. Due to the elastomers not exhibiting ideal stress–strain behaviour, the gradient of each trace is hereby referred to as the 'bulk modulus'.

At 25 °C, the materials prepared using an Sn(II) curing mechanism (Sn1, Sn3, Sn10) and the pyrene-labelled block copolymer PHMS-Py$_x$ exhibited larger bulk moduli than the Pt(0) catalysed elastomers (Pt12, Pt13, Pt15), suggesting significantly mechanically stiffer materials (Fig. 2). The Sn(II) cured materials also show the most 'ideal' stress–strain traces which may be due to the significantly longer PDMS chains used (M_w 26 000) and the increased efficiency of the catalyst. Noticeable increases in hysteresis and the bulk modulus were observed for the elastomer with a low pyrene loading (0.01 wt%, Sn1) when compared to the 'blank' PHMS control (0 wt%, Sn10). However, at a higher loading (0.1 wt%, Sn3) hysteresis decreased and the

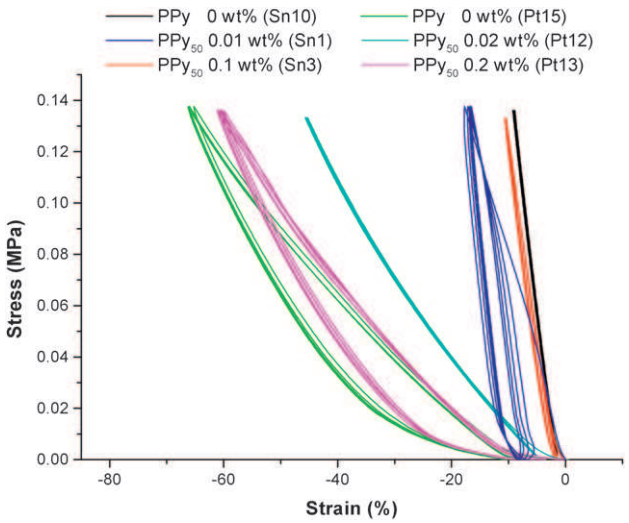

Fig. 2 Stress–strain plots from DMA of PHMS-Py$_x$ containing elastomers measured at 25 °C.

elastomer had a similar stiffness to Sn10. The reason for this remains unclear. The Pt(0) cured materials show the opposite trend to the Sn(II) cured materials. An increase in the loading of the siloxane copolymer (from 0 wt% to 0.02 wt%) caused an initial decrease in the amount of observed hysteresis and decrease in the bulk modulus associated with the stress–strain curves. A higher loading (0.2 wt%, Pt13) led to a return of significant hysteresis and a decrease in stiffness similar to that of the blank sample (Pt15). An explanation for this is not clear and more extensive testing needs to be performed on a wider range of elastomers.

The elastomers containing Py-TEOS as a cross-linking component (Fig. 3) were similar to the Sn(II)-cured elastomers incorporating the pyrene copolymers. The materials produced were stiff and displayed little hysteresis with the notable exception of Sn6 which had a low loading of the pyrene component (0.01 wt%). The incorporation of a low loading of the pyrene component led to noticeable hysteresis and increase in plasticity. However, the properties of the elastomers recovered towards the

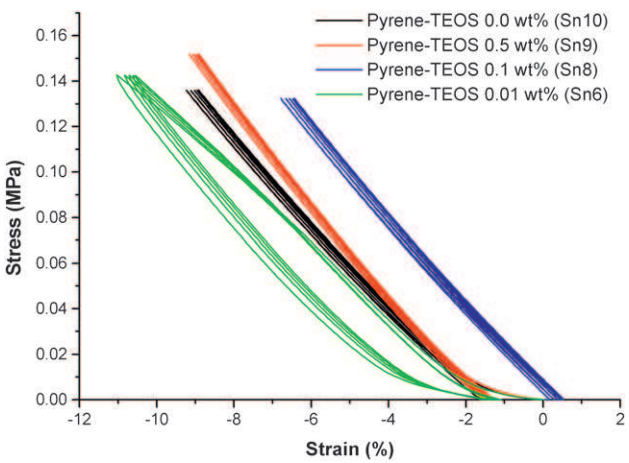

Fig. 3 Stress–strain plots from DMA of Py-TEOS containing elastomers measured at 25 °C.

values of the 'blank' elastomer (Sn10) as higher loadings of Py-TEOS (Sn8, Sn9) were incorporated.

Furthermore, the materials show some evidence of compression set, which is a progressive shift of the compression–release cycle towards more negative strain values. When stress–strain curves were measured at 40 °C, all of the materials exhibited the same general trends in bulk moduli and stress–strain behaviour as shown by the data collected at 25 °C (see ESI†, Fig. S4). However, due to the increase in temperature the materials began to show increased evidence of compression set and hysteresis, and therefore softening.

3.7 Thermal analysis

In order to determine the comparative effects of pyrene present within the siloxane elastomers, DSC analysis was performed on a number of elastomers. Glass transition temperatures (T_g), exothermic, and endothermic peaks were observed at approximately −120 °C, −90 °C, and −45 °C, respectively, in a number of samples (Fig. 4, ESI†, Table S1). Sn(II) cured elastomers (Sn1, Sn3, Sn6, and Sn8) show a T_g at −116 to −117 °C which is characteristic for PDMS elastomers.[27] However, the Pt(0) cured elastomers (Pt12, Pt13, and Pt15) did not show strong, distinct T_gs at this temperature. This is a consequence of the use of low molecular weight PDMS (M_w 186) in these materials compared to the high molecular weight PDMS (M_w 26 000) used in the Sn(II) materials. As has been observed previously,[27,28] a strong 'cold crystallisation' peak (exotherm) was also observed for the Sn(II) cured samples from −85 to −92 °C corresponding to the polymer chains orientating and forming crystalline regions within the sample. However, no obvious cold crystallisation peak was observed for Sn10 (0 wt% pyrene), despite an endothermic transition at −48 °C indicating that the sample contained significant crystalline regions. Crystallisation appears to have been inhibited during the cooling process (prior to the first heating run shown in Fig. 4) by the presence of the pyrene in comparison to the sample containing no pyrene. Comparing samples Sn1 and Sn3 which contain 0.01 wt% and 0.1 wt% PHMS-Py_{50}, respectively, there is a small increase (from −88 to −85 °C) in the cold crystallisation temperature as the pyrene content is increased. Likewise, samples Sn6 and Sn8 (0.01 wt% and 0.1 wt% pyrene-containing cross-linker, respectively) show a similar increase (−92 to −89 °C) with increasing pyrene content. This may be due to the fact that the pyrene disrupts the crystallinity of the PDMS network. Previous studies have shown that the cold crystallisation temperatures of siloxane elastomers decreased with increasing silica content due to the introduction of internal stresses and the presence of crystals.[29] Melting (endothermic) peaks were observed for all of the Sn cured samples at approximately −48 °C, near identical to the 'blank' Sn10. The Pt12 containing PHMS-Py_{50} displayed a very small cold crystallisation peak and Pt13 displayed no crystallisation peak. These samples also showed no deviation from the amorphous melting peak of the 'blank' elastomer (Pt15) at −42 °C. As expected, and in contrast to the elastomers, the pyrene-containing cross-linker (Py-TEOS) and the pyrene-containing polysiloxane precursor (PHMS-Py_{50}) showed no exo- or endothermic peaks. For PHMS-Py_{50}, a small T_g was observed at −121 °C.

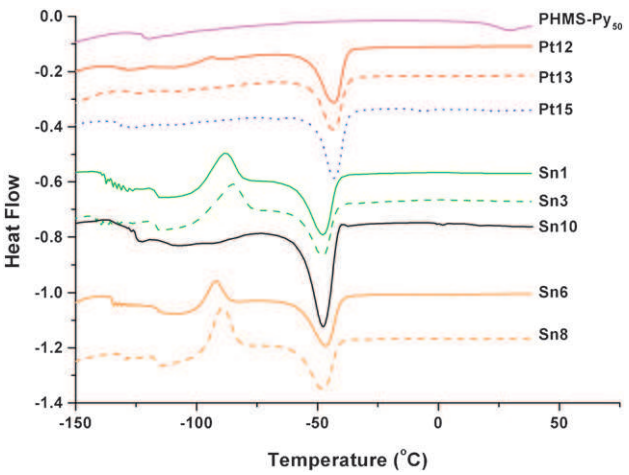

Fig. 4 First DSC heat runs recorded for various pyrene-labelled elastomers.

3.8 Photoluminescent characterisation

Pyrene forms excimers when an excited state pyrene molecule interacts with another molecule in the ground state. The excimer emission spectrum is broad, featureless, and bathochromically shifted (480 nm) compared to the photon emitted by an excited state monomer (390 nm). The advantages of using pyrene in such systems are based upon its sensitivity to its immediate environment since the wavelength of the excimer emission peak depends on its solubility in a medium (local polarity) and its interaction with other pyrene molecules (concentration). For example, it is possible to observe the excimer peak associated with pyrene at low concentrations in ethanol. Conversely, pyrene molecules are kept apart and do not form dimers as readily in a solvent such as THF, and therefore the excimer peak is not observed at low concentrations.[30]

The UV-vis spectra of pyrenemethanol, 1-allyloxymethylpyrene, and the PHMS-Py_x copolymers all exhibited characteristic absorbance peaks at 314, 328, and 344 nm due to the pyrene moiety (ESI†, Fig. S5). As expected, the 1-allyloxymethylpyrene was photoluminescent in solution; at low concentrations (1×10^{-6} mol dm^{-3}) a characteristic peak (λ_{max} 390 nm) associated with the π–π^* transitions of the monomeric form of pyrene is observed. At higher concentrations, a broader peak with λ_{max} of 480 nm corresponding to the excimer is present (Fig. 5). Intermediate concentrations gave spectra displaying both peaks.

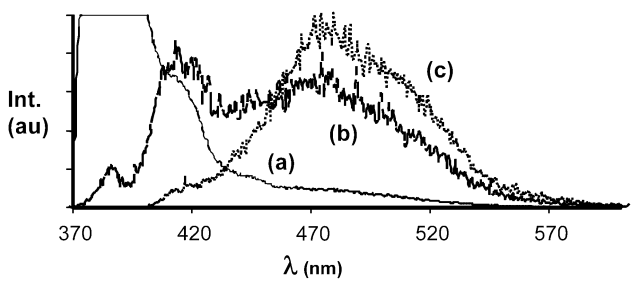

Fig. 5 Photoluminescent spectra for allyloxymethylpyrene in THF: (a) 1×10^{-6} mol dm^{-3}, (b) 1×10^{-3} mol dm^{-3} and (c) 1×10^{-2} mol dm^{-3}.

In contrast, the emission spectra for the PHMS-Py_{50} and PHMS-Py_{100} all displayed the broad absorption due to excimer formation even at very low concentrations (5×10^{-8} mol dm^{-3}) with minimal emission due to the monomeric pyrene. As an example, the excitation and emission spectra for PHMS-Py_{80} are shown in Fig. 6. Since π–π transitions are not expected for pyrene below a concentration of 1×10^{-6} in CH_2Cl_2, it follows that excimer formation must be due to intramolecular aggregation, *i.e.* the interaction between pyrene moieties present on the same polymer chain.

All of the prepared elastomer samples containing pyrene displayed photoluminescent behaviour upon excitation at 343 nm. As expected, the Sn catalysed elastomers derived from pyrene–siloxane copolymers showed a major pyrene excimer emission peak at 480 nm, with a small monomer emission peak at 390 nm

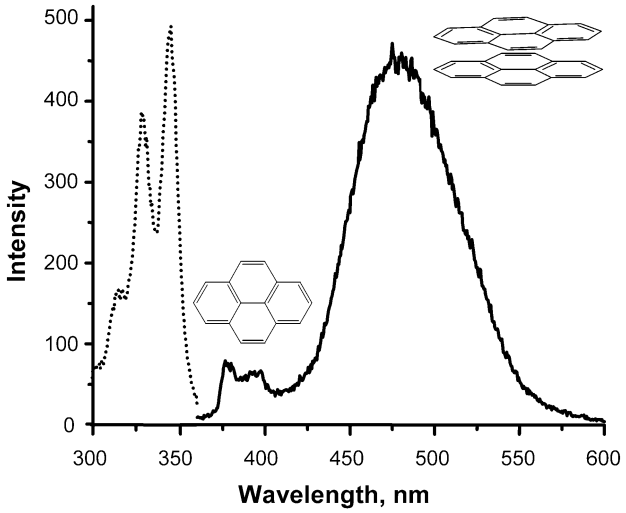

Fig. 6 Excitation (···, $\lambda_{em} = 483$ nm) and emission (—, $\lambda_{ex} = 343$ nm) spectra for PHMS-Py_{80} in THF, 1×10^{-7} mol dm^{-3}.

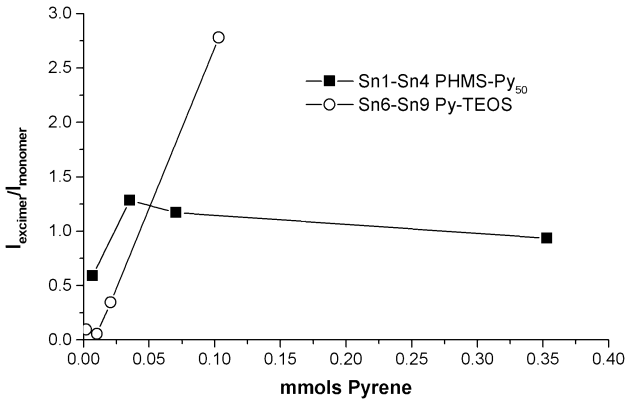

Fig. 8 Ratios of photoluminescent maximum intensities of excimer (I_{exc}) and monomer (I_{mon}) peaks for varying quantities of pyrene in PHMS-Py50 and Py-TEOS elastomer formulations.

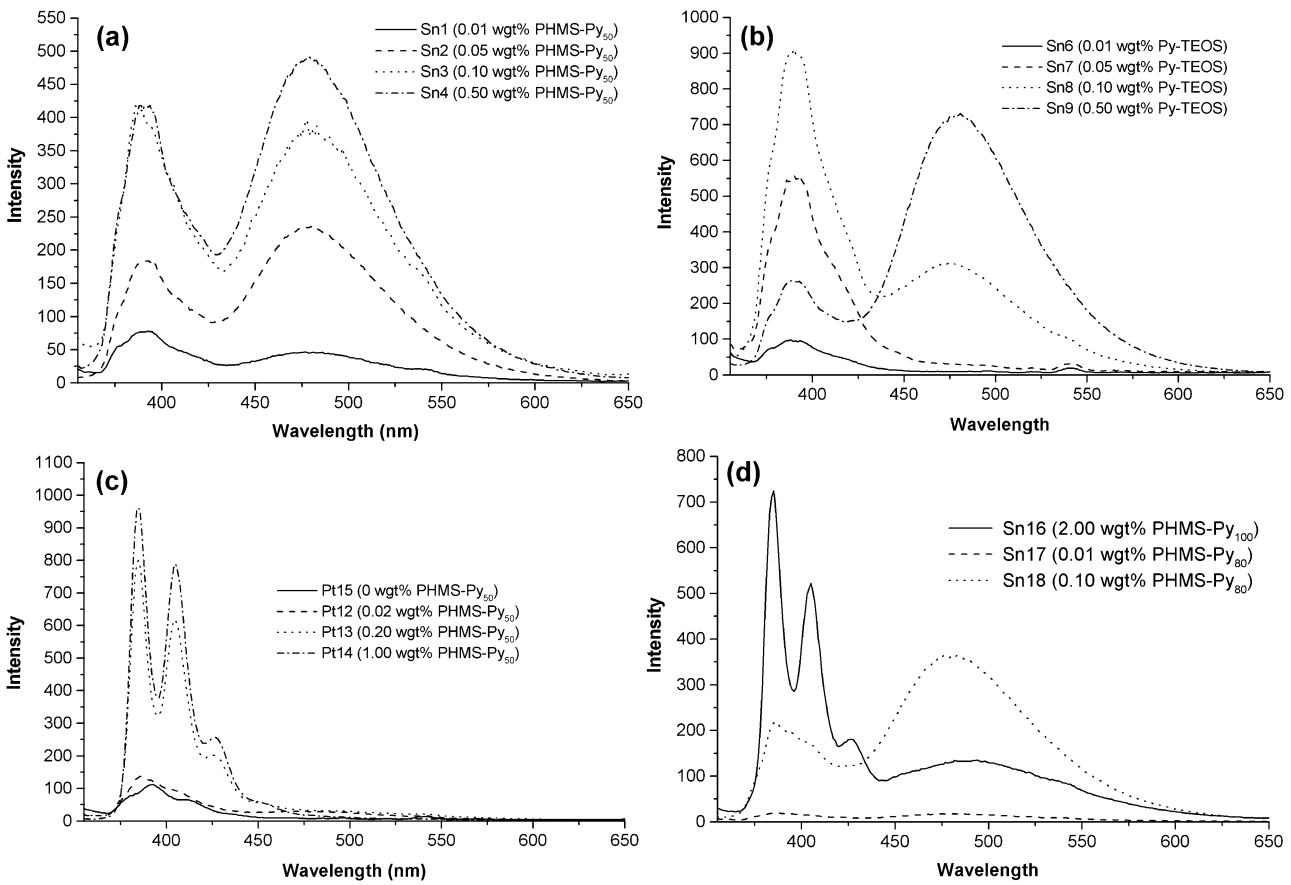

Fig. 7 Photoluminescent emission spectra for ($\lambda_{ex} = 343$ nm) the pyrene-containing elastomers.

(Fig. 7a and d). The 'blank' Sn catalysed elastomer, Sn10, formed without a pyrene–siloxane copolymer or Py-TEOS showed no fluorescence emission over the observed range (355–650 nm). For the PHMS-Py_{50} containing Sn catalysed samples Sn1–Sn4 (Fig. 7a) the intensity ratio of the excimer : monomer peaks was not proportional to the weight of PHMS-Py_{50} (and therefore concentration of Py) in the sample formulations (Fig. 8). Again this is indicative of intramolecular excimer formation. The formation and hence photoluminescent intensity of pyrene excimers should be directly proportional to concentration (see the results for Sn6–Sn9). The fact that the monomer intensities of Sn3 and Sn4 were nearly identical indicates that a certain portion of the pyrenes on the PDMS chains may be inhibited from forming excimers at all irrespective of concentration, *i.e.* the bonding of the pyrene moieties onto a PDMS chain may actually inhibit excimer formation, though this remains speculation.

In contrast to the intensity ratios of the excimer : monomer peaks for Sn1–Sn4, the Py-TEOS containing sample appeared to show that excimer formation in these elastomers was directly proportional to the mmol of pyrene (and hence concentration) included in the elastomer formulation. The excimer emissions in these samples must arise from paired pyrenes attached to separate sites within the network. Whilst only four values for I_{exc}/I_{mon} were obtained it would appear that the excimer concentration increases linearly with concentration as expected.

The Pt-catalysed samples, Pt12, Pt13 and Pt14, displayed unusual photoluminescent spectra in that only weak fluorescence due to excimer formation was visible (Fig. 7c). Furthermore in contrast to the Sn catalysed samples the vibrational structure for the pyrene monomer peaks was clearly visible with the I1, I2 and I3 bands clearly discernible. The low intensity of the excimer emission, despite the existence of intermolecular excimers for the isolated polymer chains themselves and in the Sn1–Sn4 samples, is highly curious. Two possibilities exist: (i) the elastomer environment from the Pt-catalysed systems (with their very short PDMS chains) constricts intramolecular and intermolecular aggregation of the pyrene luminophores (perhaps by inducing a fully extended conformation in the PHMS-Py_{50} chains); (ii) the excimer emission is being quenched. Given that the chemistry/structure of the elastomers themselves is not radically different from the Sn catalysed samples it is most likely that the Pt catalyst itself is causing quenching of excimer emission (both Pt^{2+} and platinum colloids are known to exist at the end of the hydrosilylation reaction).[31] Pt nano-particles have been demonstrated to quench the luminescence of a number of fluorophores and it is not unknown for Pt^{2+} complexes to also act as quenchers.[32] Whilst quenching may or may not be a result of the Pt in the sample it must be viewed as a contender for the cause of the absence of excimer fluorescence. However, this is speculation at present and this area needs further investigation to determine whether conformational/mobility effects are inhibiting excimer formation or emission is being quenched. The 'blank' Pt-catalysed pyrene-free elastomer, Pt15, displayed limited emission over the range 350–450 nm; the origin of this is unclear but is tentatively ascribed to residual platinum species in the sample.

Two elastomer samples containing PHMS-Py_{80} were prepared (Sn17, Sn18) and these displayed fluorescence spectra broadly similar to those observed for the equivalent PHMS-Py50 samples (Sn1–Sn4). Interestingly the sample prepared using PHMS-Py_{100} (which possesses no significant Si–H bonding sites) displayed both excimer and monomer peaks with the latter displaying a similar resolution of the vibrational fine structure to that observed for Pt13 and Pt14. No immediate explanation is available for this difference. Little can be surmised about the mobility or conformation of the polymer chain itself at present, *i.e.* whether reduced (or increased) mobility gives rise to the resolved vibrational fine structure. The covalently bonded nature of the PHMS-Py_x and Py-TEOS samples and their resistance to leaching of the pyrene from the material even under adverse conditions (*e.g.* in the presence of heat and organic solvent) were demonstrated by performing a Soxhlet extraction with THF on Sn7 (Py-TEOS), Pt13 (PHMS-Py_{50}) and Sn16 (PHMS-Py_{100}). For Sn7 and Pt13 the photoluminescent spectra before and after extraction were nearly identical (ESI†, Fig. S6); for Sn16 which contained PHMS-Py_{100}, which was not bound to the elastomer matrix, a significant reduction in photoluminescent intensity was observed (to less than 25% of initial value). This is a consequence of leaching of pyrene-containing material from the silicone matrix aided by THF solvation.

3.9 Photoluminescent behaviour under stress

As the stretching of a polysiloxane film occurs, a conformational change and an unravelling phenomenon take place.[33] When a polymer containing intermittently spaced pyrene substituents is stretched, the orientation and degree of overlapping of the pyrene moieties should also change. For example, if an overall effective decrease in π-stacking (excimer π–π interaction) occurs, this should manifest itself in the decrease in dimer formation (480 nm) and a relative increase in monomer abundance (~390 nm). To monitor the effects of stretching, two elastomer samples were mounted into an extensometer fitted inside a fluorimeter. The set-up of the extensometer and fluorimeter is illustrated schematically in Fig. 9. The extensometer was graded in 0.5 mm increments and stretching of the

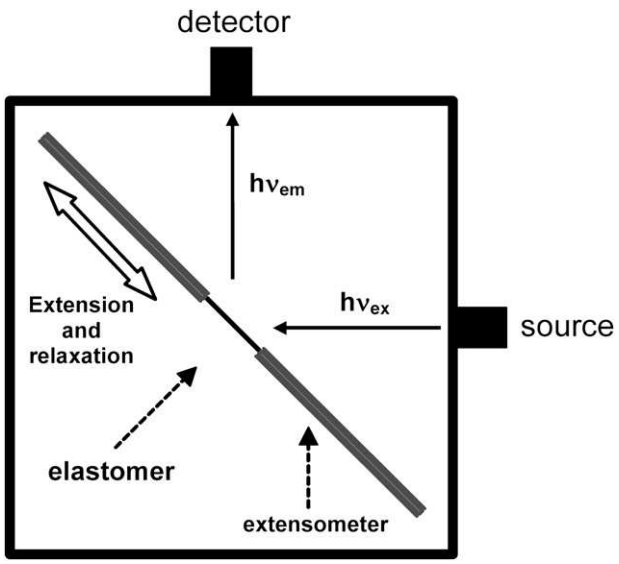

Fig. 9 Illustration of extensometer set-up inside the fluorescent spectrophotometer.

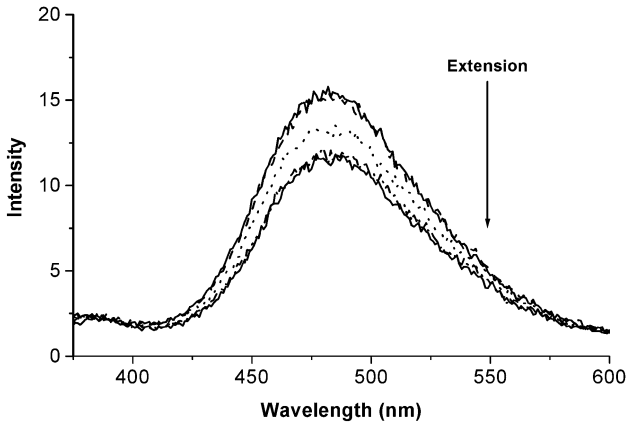

Fig. 10 Change in emission spectrum of Pt12 (0.02 wt% PHMS-Py_{50} in PDMS elastomer) with stretching to 2.0 mm (13.3% strain) at 0.5 mm increments.

elastomers was performed by increasing and decreasing the extension in 0.5 mm increments up to a maximum of 3 mm; the region of the elastomer between the clamps was 15 mm and hence the maximum extension was 20%. As the elastomers were extended and then relaxed the fluorescence emission spectra were recorded (excitation at 343 nm). Pt12 was chosen as an example of a PHMS-Py_x containing PDMS elastomer and the resultant spectra are overlaid in Fig. 10. As the sample was stretched, the wavelength intensity at 480 nm (excimer) was observed to decrease. This may be due to the decrease in elastomer thickness, and therefore path length leading to a decrease in the effective concentration of pyrene in the beam. However, for this elastomer (synthesised from the pyrene-containing copolymer) these changes in intensity with stretching were weak if at all discernable. Furthermore the intensities were patchy across the sample and difficult to reproduce. Therefore, while Pt12 showed a change upon stretching, in this case, these results were not reproducible since illumination of a different portion of the elastomer leads to no significant change in intensity when stretched. Overall it appears that this type of elastomer was not suitable for photoluminescent sensing of strain; interpretation of any photoluminescent change would also be complicated by the residual Pt luminescence (observed for Pt15).

In contrast to the pyrene-containing polymer sample, a Py-TEOS labelled elastomers (Sn9) displayed a significant increase in excimer emission (λ_{max} = 480 nm) intensity with stretching and decrease in emission intensity with relaxation (Fig. 11). This effect was reproducible over the sample surface, although the initial intensities still varied slightly at different sites. The changes in initial intensity are probably due to slight changes in the angle of incidence of the excitation and emission beams (the extensometer set-up did not allow for precise control over this variable). There may also be small variations in pyrene concentration throughout the sample. Studies are in progress to investigate these possibilities. Fig. 12 illustrates the average change in intensity (normalised to the intensity of emission at zero extension) shown over 3 stretching and recovery cycles of Sn9; no significant hysteresis was observed within the range of experimental error. Furthermore after 12 months storage significant changes in intensity with extension and relaxation

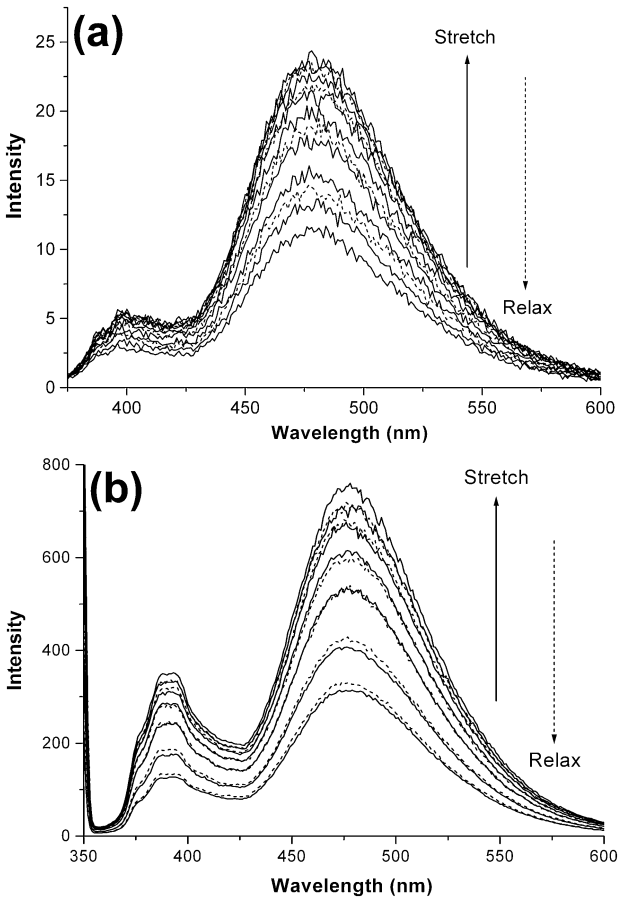

Fig. 11 Change in emission spectra of (a) Sn9 and (b) Sn9a (0.5 wt% Py-TEOS) with stretching (to 3.0 mm, 16.7% strain) and relaxation at 0.5 mm increments.

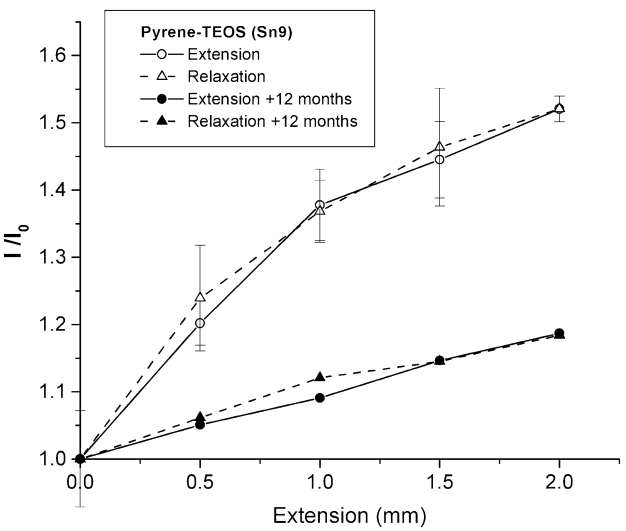

Fig. 12 Changes in photoluminescent emission intensity ratios (I = emission at increment x and I_0 = intensity in relaxed state) for Sn9 through 3 extension and relaxation cycles and the same sample after 12 months storage under argon. 2 mm = 13.3% strain.

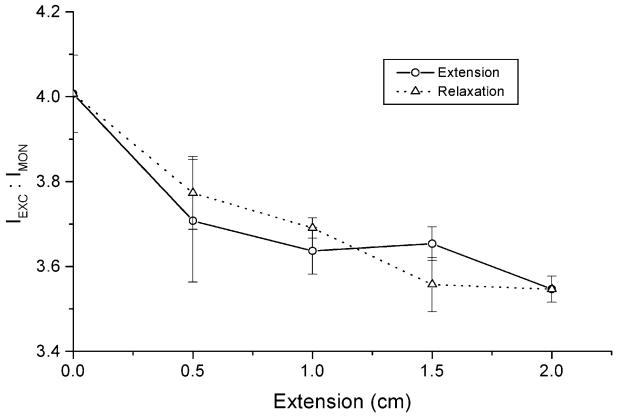

Fig. 13 Variation in the ratios of excimer (I_{exc}) to monomer (I_{mon}) pyrene photoluminescent intensities at λ_{max} with extension and relaxation over 3 cycles. 2 mm = 13.3% strain.

were still observed, though significant decrease in response to deformation was observed, however, these changes could be a result of changes in experimental set-up. Further studies are underway to ascertain long-term stability of the fluorescent response in these systems. A further sample of Sn9 was synthesised (Sn9a) and this displayed similar changes in intensity with extension and relaxation (Fig. 11b). Intriguingly the ratio of excimer to monomer emission actually decreased with stretching (Fig. 13), indicating that the abundance of the monomeric pyrene is increasing in relation to the excimer concentration upon the application of stress. More detailed and careful studies are underway to determine what might cause this behaviour in the Py-TEOS elastomer. A possible explanation would be a significant re-orientation of the pyrene moieties in the elastomer with deformation. Whilst initially randomly aligned, upon stretching a degree of alignment was induced across the pyrene molecules and the total area capturing incident excitation light increases. Furthermore the decrease in the intensity of the excitation peak corresponding to the excimer peak relative to the monomer excitation peak indicates that excimer pairs are being disrupted resulting in a relative increase in monomer concentration.

4. Conclusions

The synthesis of allyl-functionalised pyrene provided an efficient route to pyrene-substituted polysiloxanes. A range of copolymers with varying degrees of pyrene content were synthesised; the remaining unconjugated Si–H sites were employed as cross-linking sites in order to incorporate the copolymers into the siloxane elastomer networks. The networks were formed *via* either Sn(II) catalysed condensation or Pt(0) catalysed hydrosilylation reactions. As the pyrene–siloxane copolymer content increased, the elastomers became less homogeneous, more opaque, and in some cases where Pt(0) was used to cross-linked elastomers, bubbles tended to form. In a more successful approach a pyrene-labelled cross-linker molecule was synthesised possessing a triethoxysilane moiety suitable for acting as a cross-linker site in an Sn(II) cured elastomer. Importantly, preliminary experiments indicated that the incorporation of pyrene (either bound to a polymer or at a cross-linking site) did not significantly alter the thermal or mechanical properties of the elastomer.

Fluorescence spectroscopy showed that the elastomers displayed excimer emission peaks indicative of pyrene dimers, and in some cases also gave emission peaks corresponding to pyrene monomers. By stretching certain elastomers to various degrees inside a fluorimeter, it was possible to detect changes in emissions at 390 nm and 480 nm. A pyrene–polysiloxane copolymer containing elastomer gave some results demonstrating variations in intensity with deformation, although these results varied depending on the site of emission of the elastomer and were not reproducible. The alternative method of chemically bonding pyrene at cross-linking sites within the elastomers also proved successful in synthesising fluorescent PDMS elastomers. The emission peaks displayed by these materials gave reproducible variations in intensity with extension and relaxation of the elastomers. Coupled with the maintenance of similar physical properties to the blank elastomer (containing no pyrene) this provides a promising route for the *in situ* non-invasive method of monitoring strain in silicone elastomers and possibly ultimately calibrating emission intensity with deformation. Further detailed results and in-depth discussion of the response of the pyrene-labelled elastomers to stress (such as fluorophore orientation, scaling of response with strain, homogeneity of fluorophore distribution, 2D imaging for example) will be presented in a forthcoming publication. In addition, a detailed correlation of mechanical and thermal properties with pyrene concentration and prolonged cycling studies will be investigated.

Acknowledgements

We thank the EPSRC for support from a DTA and CASE award for D. R. T. Roberts.

References

1 (*a*) C. W. Tang, *US Pat.*, 4 356 429, 1982; (*b*) S. A. Van Slyke, C. W. Tang, *US Pat.*, 4 539 507, 1985; (*c*) C. W. Tang, C. H. Chen, *US Pat.*, 4 769 292, 1988.
2 J. Bisberg, W. J. Cumming, R. A. Guadiana, K. D. Hutchinson, R. T. Ingwall, E. S. Kolb, P. G. Mehta, R. A. Minns and C. P. Petersen, *Macromolecules*, 1995, **28**, 386.
3 B. J. Basu, A. Thirumurugan, A. R. Dinesh, C. Anandan and K. S. Rajam, *Sens. Actuators, B*, 2005, **104**, 15.
4 B. J. Basu, N. Vasantharajan and C. Raju, *Sens. Actuators, B*, 2009, **138**, 283–288.
5 F. Lu, L. Gao, L. Ding, L. Jiang and Y. Fang, *Langmuir*, 2006, **22**, 841.
6 T. Ikawa, T. Shiga and A. Okada, *J. Appl. Polym. Sci.*, 1997, **66**, 1569.
7 H. Spanggaard, M. Jorgensen and K. Almdal, *Macromolecules*, 2003, **36**, 1701.
8 D. Olmos, A. J. Aznar, J. Gonzalez-Benito and J. Baselga, *J. Mater. Process. Technol.*, 2003, **143**, 495.
9 J. Vandendriessche, P. Palmans, S. Toppet, N. Boens, F. C. De Schryver and H. Masuhara, *J. Am. Chem. Soc.*, 1984, **106**, 8057.
10 K. D. Belfield, C. Chinna and O. Najjar, *Macromolecules*, 1998, **31**, 2918.
11 S. J. Clarson, in *Silicon-Containing Polymers*, ed. R. G. Jones, W. Ando and J. Chojnowski, Kluwer Academic Publishers, Dordrecht, 2000, ch. 5, p. 139.
12 F. B. Dias, J. C. Lima, A. L. Macanita, S. J. Clarson, A. Horta and I. F. Pierola, *Macromolecules*, 2000, **33**, 4772.
13 I. Toulokhonova, B. Bjerke-Kroll and R. West, *J. Organomet. Chem.*, 2003, **686**, 101.
14 S. D. Kim and J. M. Torkelson, *Macromolecules*, 2002, **35**, 5943.

15 M. Wilhelm, C.-L. Zhao, Y. Wang, R. Xu, M. A. Winnik, J.-L. Mura, G. Riess and M. D. Croucher, *Macromolecules*, 1991, **24**, 1033.
16 J. Aguiar, P. Carpena, J. A. Molina-Bolivar and C. Carnero Ruiz, *J. Colloid Interface Sci.*, 2003, **258**, 116.
17 M. Szadkowska-Nicze, M. Wolszczak, J. Kroh and J. Mayer, *J. Photochem. Photobiol., A*, 1993, **75**, 125.
18 R. B. Crenshaw and C. Weder, *Chem. Mater.*, 2003, **15**, 4717.
19 A. Avis and G. Porter, *J. Chem. Soc., Faraday Trans. 2*, 1974, **70**, 1057.
20 G. E. Johnson, *Macromolecules*, 1980, **13**, 839.
21 T. Keeling-Tucker and J. D. Brennan, *Chem. Mater.*, 2001, **13**, 3331.
22 (*a*) B. J. Basu, C. Anandan and K. S. Rajam, *Sens. Actuators, B*, 2003, **94**, 257; (*b*) C. Anandan, B. J. Basu and K. S. Rajam, *Eur. Polym. J.*, 2004, **40**, 335; (*c*) B. J. Basu and K. S. Rajam, *Sens. Actuators, B*, 2004, **99**, 459; (*d*) Y. Le Sant and M.-C. Merienne, *Aerosp. Sci. Technol.*, 2005, **9**, 285.
23 B. P. S. Chauhan, T. E. Ready, Z. Al-Badri and P. Boudjouk, *Organometallics*, 2001, **20**, 2725.
24 (*a*) J. L. Speier, *Adv. Organomet. Chem.*, 1979, **17**, 407; (*b*) J. N. Lewis, *J. Am. Chem. Soc.*, 1991, **112**, 5998.
25 R. Metivier, I. Leray, M. Roy-Auberger, N. Zanier-Szydlowski and B. Valeur, *New J. Chem.*, 2002, **26**, 411.
26 D. R. Thomas, in *Siloxane Polymers*, ed. S. J. Clarson and J. A. Semlyen, Prentice Hall, Englewood Cliffs, NJ, 1993, p. 567.
27 A. Shefer and M. Gottlieb, *Macromolecules*, 1992, **25**, 4036.
28 M. I. Aranguren, *Polymer*, 1998, **20**, 4897.
29 A. Yim and L. E. St. Pierre, *J. Polym. Sci., Part B: Polym. Lett.*, 1970, **8**, 241.
30 D. C. Dong and M. A. Winnik, *Photochem. Photobiol.*, 1982, **35**, 17.
31 J. Stein, L. N. Lewis, Y. Gao and R. A. Scott, *J. Am. Chem. Soc.*, 1999, **121**, 3693–3703.
32 (*a*) B. Wang, K. Chen, S. Jiang, F. Reincke, W. J. Tong, D. Y. Wang and C. Y. Gao, *Biomacromolecules*, 2006, **7**, 1203–1209; (*b*) E. J. New, R. Duan, J. Z. Zhang and T. W. Hambley, *Dalton Trans.*, 2009, 3092–3101.
33 J. E. Mark, *Prog. Polym. Sci.*, 2003, **28**, 1205.

